Development/Plasticity/Repair

Upregulation of Sodium Channel $Na_v1.3$ and Functional Involvement in Neuronal Hyperexcitability Associated with Central Neuropathic Pain after Spinal Cord Injury

Bryan C. Hains, Joshua P. Klein, Carl Y. Saab, Matthew J. Craner, Joel A. Black, and Stephen G. Waxman

Department of Neurology and Paralyzed Veterans of America/Eastern Paralyzed Veterans Association Neuroscience Research Center, Yale University School of Medicine, New Haven, Connecticut 06510, and Rehabilitation Research Center, Veterans Affairs Connecticut Healthcare System, West Haven, Connecticut 06516

Spinal cord injury (SCI) can result in hyperexcitability of dorsal horn neurons and central neuropathic pain. We hypothesized that these phenomena are consequences, in part, of dysregulated expression of voltage-gated sodium channels. Because the rapidly repriming TTX-sensitive sodium channel $Na_v1.3$ has been implicated in peripheral neuropathic pain, we investigated its role in central neuropathic pain after SCI. In this study, adult male Sprague Dawley rats underwent T9 spinal contusion injury. Four weeks after injury when extracellular recordings demonstrated hyperexcitability of L3–L5 dorsal horn multireceptive nociceptive neurons, and when pain-related behaviors were evident, quantitative RT-PCR, *in situ* hybridization, and immunocytochemistry revealed an upregulation of $Na_v1.3$ in dorsal horn nociceptive neurons. Intrathecal administration of antisense oligodeoxynucleotides (ODNs) targeting $Na_v1.3$ resulted in decreased expression of $Na_v1.3$ mRNA and protein, reduced hyperexcitability of multireceptive dorsal horn neurons, and attenuated mechanical allodynia and thermal hyperalgesia after SCI. Expression of $Na_v1.3$ protein and hyperexcitability in dorsal horn neurons as well as pain-related behaviors returned after cessation of antisense delivery. Responses to normally noxious stimuli and motor function were unchanged in SCI animals administered $Na_v1.3$ antisense, and administration of mismatch ODNs had no effect. These results demonstrate for the first time that $Na_v1.3$ is upregulated in second-order dorsal horn sensory neurons after nervous system injury, showing that SCI can trigger changes in sodium channel expression, and suggest a functional link between $Na_v1.3$ expression and neuronal hyperexcitability associated with central neuropathic pain.

Key words: **ion channel; sensitization; contusion; trauma; wide dynamic range; pain**

Introduction

Most patients with traumatic spinal cord injury (SCI) report moderate to severe chronic pain that is refractory, or only partially responsive, to standard clinical interventions (Balazy, 1992; Turner et al., 2001). Experimental contusion SCI in rodents can produce long-lasting central neuropathic pain (Hulsebosch et al., 2000; Lindsey et al., 2000; Hains et al., 2001; Mills et al., 2001). In spinally injured animals, alterations in electrophysiologic properties of dorsal horn neurons (Hao et al., 1991; Yezierski and Park, 1993; Drew et al., 2001; Hains et al., 2003a,b) are thought to contribute to changes in somatosensory responsiveness.

Voltage-gated sodium channels (VGSCs) are responsible for the generation and propagation of action potentials in neurons, and various subtypes of these channels are expressed in specific spatial and temporal patterns at different stages of development. The TTX-sensitive (TTX-S) $Na_v1.3$–brain type III sodium channel is expressed at relatively high levels in embryonic dorsal root ganglion (DRG) neurons but is barely detectable in adult DRG neurons (Waxman et al., 1994; Felts et al., 1997). Its expression is similarly decreased in the adult spinal cord and CNS throughout development (Beckh et al., 1989; Brysch et al., 1991; Furuyama et al., 1993; Felts et al., 1997; Hains et al., 2002).

After peripheral nerve injury, altered regulation of VGSC expression results in hyperexcitability of injured primary spinal sensory neurons that contributes to neuropathic pain (Matzner and Devor, 1992; Devor, 1994; Waxman et al., 1999). Upregulated expression of $Na_v1.3$ mRNA and protein occurs in DRG neurons of adult rats after axotomy of their peripheral projections (Waxman et al., 1994; Dib-Hajj et al., 1996; Black et al., 1999), after chronic constriction injury (Dib-Hajj et al., 1999), and after tight spinal nerve ligation (Kim et al., 2001), producing a rapidly repriming TTX-S current that permits neuronal firing at higher than normal frequencies (Cummins and Waxman, 1997; Cummins et al., 2001).

Although hyperexcitability of dorsal horn neurons is well documented after experimental SCI and is associated with allodynia

Received June 16, 2003; revised July 30, 2003; accepted July 30, 2003.

This work was supported in part by grants from the Medical Research Service and Rehabilitation Research Service, Department of Veterans Affairs. We also thank the Eastern Paralyzed Veterans Association and the Paralyzed Veterans of America for their support. B.C.H. was funded by The Christopher Reeve Paralysis Foundation (HB1-0304-2) and National Institutes of Health–National Institute of Neurological Disorders and Stroke (1 F32 NS046919-01). We thank Dr. Sulayman Dib-Hajj for guidance in design of oligodeoxynucleotides and PCR primers and Bart Toftness for excellent technical assistance.

Correspondence should be addressed to Dr. Stephen G. Waxman, Department of Neurology, LCI-707, Yale School of Medicine, 333 Cedar Street, New Haven, CT 06510. E-mail: stephen.waxman@yale.edu.

 0270-6474/03/238881-12$15.00/0

and hyperalgesia, little is known about the molecular mechanisms underlying the neuronal hyperexcitability and pain-related behaviors. Thus, we hypothesized that an increase in expression of $Na_v1.3$, similar to the changes in DRG neurons after peripheral axotomy, takes place in lumbar dorsal horn sensory neurons after SCI. To test this hypothesis, we examined $Na_v1.3$ expression in these cells and, using targeted antisense (AS) oligodeoxynucleotide (ODN) knock-down strategies, examined the functional contribution of $Na_v1.3$ to hyperexcitability of dorsal horn neurons and central neuropathic pain after SCI.

Materials and Methods

Animal care. Experiments were performed in accordance with National Institutes of Health guidelines for the care and use of laboratory animals, and all animal protocols were approved by the Yale University Institutional Animal Care and Use Committee. Adult male Sprague Dawley rats (200–225 gm) were used for this study. Animals were housed under a 12 hr light/dark cycle in a pathogen-free area with *ad libitum* access to water and food.

Spinal cord contusion injury. Rats ($n = 74$) were deeply anesthetized with ketamine/xylazine (80/5 mg/kg, i.p.). Spinal contusion injury ($n = 57$) was produced at spinal segment T9 using the MASCIS/NYU impact injury device (Gruner, 1992; Huang and Young, 1994). A 10 gm, 2.0 mm diameter rod was released from a 25 mm height onto the exposed spinal cord, resulting in a mean tissue compression of 1.96 ± 0.18 mm. For sham surgery, animals ($n = 17$) underwent laminectomy and placement into the vertebral clips of the impactor only. After SCI or sham surgery, the overlying muscles and skin were closed in layers with 4-0 silk sutures and staples, respectively, and the animal was allowed to recover on a 30°C heating pad. Postoperative treatments included saline (2.0 cc, s.c.) for rehydration, and Baytril (0.3 cc, 22.7 mg/ml, s.c., twice daily) to prevent urinary tract infection. Bladders were manually expressed twice daily until reflex bladder emptying returned, typically by 10 d after injury. After surgery, animals were maintained under the same preoperative conditions, and fed *ad libitum*.

ODN synthesis and delivery. In animals ($n = 57$) 28 d after SCI, under ketamine/xylazine (80/5 mg/kg, i.p.) anesthesia, a sterile premeasured 32 ga intrathecal catheter (ReCathCo, Allison Park, PA) was introduced through a slit in the atlanto-occipital membrane, threaded down to the lumbar enlargement, secured to the neck musculature with suture, and heat sealed to prevent infection and leakage of cerebrospinal fluid. Three days after catheter placement (day 31), under brief (<1 min) halothane sedation (3% by facial mask), intrathecal administration of an AS ODN sequence corresponding to the translation initiation site of $Na_v1.3$ (5′-CAGTGCCTGGGCCATCTTTTC-3′) (SCI + AS; $n = 23$), or its mismatch (MM) (5′-CGATCGCGTGCGCTATCTTCT-3′) (SCI + MM; $n = 17$) was initiated. For 4 d, 45 μg/5 μl twice daily of either AS or MM in artificial CSF (aCSF) containing (in mM): 1.3 $CaCl_2$–$2H_2O$, 2.6 KCl, 0.9 MgCl, 21.0 $NaHCO_3$, 2.5 Na_2HPO_4–$7H_2O$, 125.0 NaCl, prepared in sterile H_2O, was injected followed by 10 μl of aCSF flush. On day 4, Cy3-tagged AS or MM was delivered in the same manner to a subset of these animals. In another group of animals (SCI + AS/WD; $n = 6$), AS injections were stopped after 4 d, and outcome measures continued for another 5 d. A separate group of injured animals (SCI; $n = 17$) underwent injection of aCSF only. Finally, a group of naive animals (N + AS; $n = 6$) received AS injections to test behavioral consequences of AS administration and to determine whether $Na_v1.3$ AS altered levels of $Na_v1.3$ in the uninjured nervous system.

By BLAST search, the antisense sequence did not show similarity, over the entire 21 nucleotides, to the sequences for any other sodium channel or to other genes; basic local alignment search tool (BLAST) search specifically demonstrated that there was no homology to $Na_v1.1$, $Na_v1.2$, or $Na_v1.6$, other Na^+ channels that are known to be expressed in dorsal horn neurons.

Locomotor function. Behavioral analysis was performed on animals from the following groups: sham-operated ($n = 10$), N + AS ($n = 6$), SCI ($n = 10$), SCI + MM ($n = 10$), SCI + AS, and SCI + AS/WD ($n = 16$). Preoperative testing began 2 d before injury and was performed weekly for 4 weeks after SCI. After this, testing was performed daily during and after cessation of ODN administration. Locomotor function was recorded by an observer blinded to the surgical status (or AS–MM status) of the animals using the Basso, Beattie, and Bresnahan (BBB) locomotor rating scale (Basso et al., 1995) to ensure reliability of hindlimb somatosensory testing and to assess treatment outcome.

Mechanical behavioral testing. The time points and sample sizes for mechanical testing were the same as those for locomotor testing. After acclimation (30 min), mechanical sensory thresholds were determined by paw withdrawal to application of a series of von Frey filaments to the glabrous surface of the paw. Calibrated von Frey filaments (Stoelting, Wood Dale, IL) in the range of 0.4–26 gm were applied with enough force to cause buckling of the filament. A modification of the "up-down" method of Dixon (1980) was used to determine the value at which paw withdrawal occurred 50% of the time (Chaplan et al., 1994), interpreted to be the mechanical nociceptive threshold. In addition, normally noxious pinprick stimuli were applied to assess changes in normal nociceptive responsiveness. Complex supraspinal behaviors such as head turning, vocalization, biting attacks on the stimulus, and whole-body postural changes excluded simple hyperreflexia, which is a segmental response (Woolf, 1984; Vincler et al., 2001).

Thermal behavioral testing. The time points and sample sizes for thermal testing were the same as those for locomotor and mechanical testing. Thermal hyperalgesia was assessed by measuring the latency of paw withdrawal in response to a radiant heat source (Dirig et al., 1997). Animals were placed in Plexiglas boxes on an elevated glass plate under which a radiant heat source (4.7 A) was applied to the glabrous surface of the paw through the glass plate. The heat source was turned off automatically by a photocell after limb lift (or at 20 sec to prevent tissue damage), allowing the measurement of paw withdrawal latency. Three minutes were allowed between each trial, and four trials were averaged for each limb. Supraspinal responses such as whole-body attention, writhing, and vocalizations accompanied paw withdrawals.

In situ *hybridization.* Tissue was collected from the lumbar enlargement (L3–L5) of animals from the following groups: sham-operated ($n = 10$), SCI ($n = 10$), SCI + MM ($n = 10$), and SCI + AS ($n = 10$). Rats were deeply anesthetized with ketamine/xylazine (80 mg/5 kg, i.p.) and perfused intracardially with 0.01 M PBS followed by 4% cold, buffered paraformaldehyde. Tissue was postfixed for 30 min in 4% paraformaldehyde and cryopreserved overnight at 4°C in 30% sucrose. Thin (12 μm) cryosections ($n = 6$ sections per animal) from different treatment groups were processed simultaneously for *in situ* hybridization cytochemistry as described previously (Black et al., 1996), except that incubation in 4% paraformaldehyde was increased to 12 min and permeabilization with proteinase K was reduced to 6 min. Briefly, sections were deproteinized with proteinase K (2.5 μg/ml), acetylated with 0.25% acetic anhydride in 0.1 M triethanolamine, and incubated in hybridization buffer (50% formamide, 10% dextran sulfate, 20 mM Tris-HCl, pH 7.5, 5 mM EDTA, 0.3 M NaCl, 0.2% SDS, 1× Denhardt's solution, 10 mM DTT) containing digoxigenin (DIG)-UTP-labeled $Na_v1.3$ riboprobe (0.5 ng/μl) for 16 hr at 58°C. After rinsing in 2× SSC, 50% formamide, and RNase solution in 0.2× SSC, slides were transferred into 100 mM Tris-HCl, pH 7.5, 150 mM NaCl, incubated in alkaline phosphatase-labeled anti-DIG antibody (1:5000 dilution in Tris-NaCl buffer) overnight at 4°C, and reacted in a chromagen solution containing 4-nitroblue tetrazolium chloride and 5-bromo-4-chloro-3-indolyl phosphate in buffer (100 mM Tris-HCl, pH 9.5, 10 mM NaCl, 50 mM $MgCl_2$), and the reaction was stopped by washing in buffer (10 mM Tris-HCl, pH 8.0, 1 mM EDTA). DIG-labeled antisense and sense riboprobes for $Na_v1.3$ (nucleotides 6335–6813; GenBank accession number Y00766) were synthesized as described previously (Black et al., 1996). Sense riboprobes yielded no signal on *in situ* hybridization (data not shown).

Quantitative RT-PCR. Fresh tissue was collected rapidly from the lumbar enlargement (L3–-L5) of animals from the following groups: sham-operated ($n = 10$), SCI ($n = 10$), SCI + MM ($n = 10$), and SCI + AS ($n = 10$), and flash frozen. Total tissue RNA was extracted using RNeasy mini-columns (Qiagen, Valencia, CA), and purified RNA was treated with RNase-free DNase-I and repurified using an RNeasy mini-column; RNA was eluted in a 50 μl volume of H_2O. First-strand cDNA was reverse

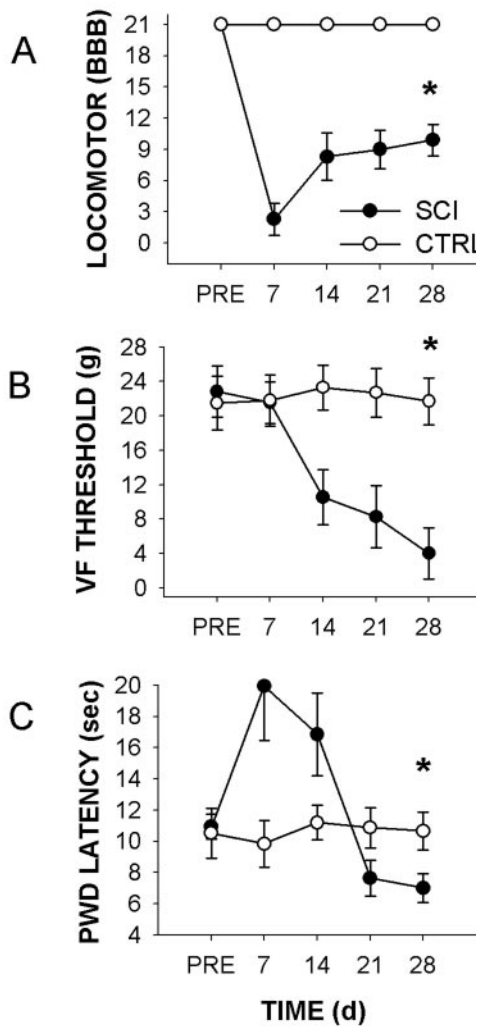

Figure 1. Behavioral changes after T9 spinal contusion SCI ($n = 10$ animals per group). Mean ± SD. BBB open-field locomotor rating scores (*A*) show spontaneous partial recovery of motor function after SCI, permitting nociceptive testing. Mean ± SD von Frey filament (VF) threshold values to hindlimb paw withdrawal (PWD) (*B*) showed that by 28 d after SCI, withdrawal thresholds significantly ($*p < 0.05$) decreased compared with sham-operated controls, indicating the development of mechanical allodynia. Mean ± SD paw withdrawal latency (seconds) to radiant thermal stimuli for hindlimbs (*C*) after SCI demonstrates significant ($*p < 0.05$) development of thermal hyperalgesia by 28 d after injury. In sham-operated animals, no differences in paw withdrawal latency were observed.

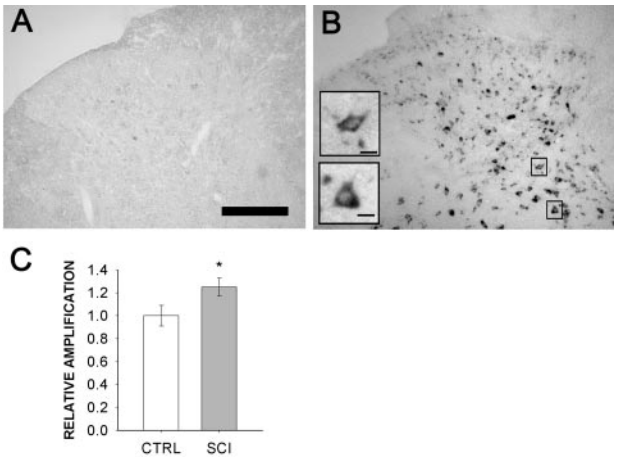

Figure 2. *In situ* hybridization for $Na_v1.3$ shows very light signal within the gray matter of the lumbar dorsal horn of sham-operated animals (*A*). In contrast, 28 d after SCI, $Na_v1.3$ hybridization signal was more intense and widely distributed throughout dorsal horn lamina I–V neurons (*B*). Higher-magnification images (*B*, inset boxes) of individual cells demonstrate neuronal morphologies and cytoplasmic staining. No labeling was observed in afferent fibers, dendritic or axonal arborizations, or white matter. Quantitative RT-PCR amplification (*C*) showed a significant ($*p < 0.05$) increase in lumbar $Na_v1.3$ mRNA in the SCI group ($n = 10$ animals) when compared with sham-operated controls (CTRL) ($n = 10$ animals). Scale bar: *A*, *B*, 300 μm; insets, 10 μm.

transcribed in a final volume of 50 μl using 5 μl purified total RNA, 1 mM random hexamer primer (Roche, Indianapolis, IN), 40 U SuperScript II reverse transcriptase (Invitrogen, Carlsbad, CA), and 40 U of RNase inhibitor (Roche). The buffer consisted of (in mM): 50 Tris-HCl, pH 8.3, 75 KCl, 3 $MgCl_2$, 10 DTT, and 5 dNTP. The reaction proceeded at 37°C for 90 min, 42°C for 30 min, and was terminated by heating to 95°C for 5 min. A parallel reaction with identical reagents but with omission of the reverse transcriptase enzyme was performed as a negative control to demonstrate the absence of contaminating genomic DNA (data not shown).

Expression of $Na_v1.3$ mRNA was quantified using the relative standard curve method of PCR. Ribosomal RNA (rRNA) (18S) was used as an endogenous control to normalize expression levels. $Na_v1.3$ cDNA was obtained from human embryonic kidney 293 cells stably transfected with a $Na_v1.3$ construct (Cummins et al., 2001). Standards and unknowns were amplified in quadruplets. Primer and probe sequences for the $Na_v1.3$ target were designed using Primer Express software (Applied Biosystems, Foster City, CA) according to the specifications of the TaqMan protocol (Winer et al., 1999). Sequences for the forward primer, reverse primer, and probe are as follows: 5′-AGGACAATGTCCAGAAGGGTAC-3′, 5′-AGTAGTCCTGAGTCATGAGTCGAAAC-3′, and 5′-TGGGACGAAACCCCAACTACGGCTACAC-3′, respectively. The amplicon comprises nucleotides 1442–1556 of the $Na_v1.3$ gene. Primers and probes were synthesized and purified by Applied Biosystems. Primers and 18S rRNA were used at a final concentration of 900 and 50 nM, respectively, whereas the probes were used at a final concentration of 200 nM. Amplification was done in a 25 μl final volume, under the following cycling conditions: 10 min at 50°C, and then 40 cycles of 95°C for 15 sec followed by 60°C for 1 min. An ABI Prism 7700 (Applied Biosystems) ran the PCR reaction, and values were obtained using Sequence Detector v1.6.3. Sodium channel and 18S rRNA templates were amplified in separate wells. The standard curves for sodium channel primer–probe sets and 18S rRNA endogenous control were constructed from the respective mean critical threshold (C_T) value, and the equation describing the curve was derived using Sequence Detection System software v1.6.3 (Applied Biosystems).

Immunocytochemistry. Tissue was collected from the lumbar enlargement (L3–L5) of animals from the following groups: sham-operated ($n = 10$), N + AS ($n = 6$), SCI ($n = 10$), SCI + MM ($n = 10$), SCI + AS ($n = 10$), and SCI + AS/WD ($n = 3$). Thin (12 μm) cryosections ($n = 5$ sections per animal) from different treatment groups were processed simultaneously. For detection of $Na_v1.3$ protein, slides were incubated at room temperature in the following: (1) blocking solution (PBS containing 5% NGS, 2% BSA, 0.1% Triton X-100, and 0.02% sodium azide) for 30 min; (2) subtype-specific primary antibody raised in rabbit against $Na_v1.3$ (Hains et al., 2002) overnight in blocking solution; (3) PBS, six times for 5 min each; (4) goat anti-rabbit IgG-Cy3 (1:2000; Amersham Biosciences, Piscataway, NJ) in blocking solution, 2 hr; and (5) PBS, six times for 5 min each. To determine whether changes in expression of $Na_v1.3$ occurred in neurons, astrocytes, and microglia, double-labeling experiments were performed with the addition of mouse anti-GFAP (1:50; Chemicon, Temecula, CA) or mouse anti-OX42 (CD11b/c) (1:200, BD Biosciences, San Jose, CA) antibodies. To identify expression of $Na_v1.3$ in nociceptive afferent fibers and dorsal horn neurons, goat anti-calcitonin gene-related peptide (CGRP) (1:500, Santa Cruz Biotechnology, Santa Cruz, CA), or guinea pig anti-neurokinin-1 receptor (NK1R) (1:250, Affiniti Research Products, Exeter, UK) primary antibodies were used. Secondary antibodies included goat anti-rabbit and anti-mouse Cy3 (1:2000, Amersham Biosciences), donkey anti-goat Alexa 488 (1:

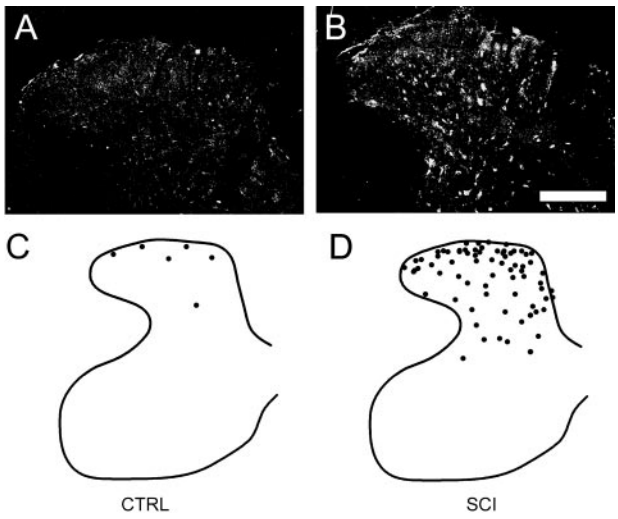

Figure 3. Immunocytochemical localization of $Na_v1.3$ protein within lumbar dorsal horn in sham-operated controls (*A*) revealed very few $Na_v1.3$ immunopositive profiles within superficial and deep laminas. Twenty-eight days after SCI (*B*), positively labeled cell profiles were observed throughout dorsal horn lamina I–V neurons. In these sections, small neurons within laminas I–II and larger neurons within laminas III–V were strongly labeled. Localization of immunopositive profiles from a number of sections ($n = 4$) plotted on a representative schematic of the lumbar spinal cord (*C*, *D*) show that after SCI, the number of profiles was increased within all laminas. The distribution of immunopositive cells was fairly homogenous and is not confined to specific laminas. Scale bar, 300 μm. CTRL, Controls.

1000, Molecular Probes, Eugene, OR), and goat anti-guinea pig Cy2 (1:250, Rockland Immunochemicals, Gilbertsville, PA). Normal horse serum replaced NGS in the blocking solution. Control experiments were performed without primary or secondary antibodies and blocking substances, which yielded only background levels of signal.

Quantitative image analysis. Images were captured with a Nikon Eclipse E800 light microscope equipped with epifluorescence and Nomarski optics, using a SPOT-RT camera (Diagnostic Instruments, Sterling Heights, MI). Quantitative microdensitometry was performed using IPLab Spectrum software (Scanalytics, Fairfax, VA). For immunocytochemistry and *in situ* hybridization experiments, the number of positively labeled neurons was counted for each dorsal horn lamina or section. Signal intensity was obtained by outlining individual neurons ($n = 15$ cells per lamina) and using IPLab integrated densitometry functions to determine levels of signal. Cells were sampled only if the nucleus was visible within the plane of section and if cell profiles exhibited distinctly delineated borders. Background levels of signal were subtracted, and control and experimental conditions were evaluated in identical manners.

Electrophysiologic procedures. Animals from sham-operated ($n = 5$), SCI ($n = 5$), SCI + MM ($n = 4$), SCI + AS ($n = 5$), and SCI + AS/WD ($n = 2$) groups underwent extracellular single unit recording according to established methods (Hains et al., 2003a,b). The activity of three to five unique cells per animal was recorded, yielding 15–25 cells per group. In the case of the SCI + AS/WD group, $n = 11$ cells were sampled. Rats were initially anesthetized with halothane (4% in induction chamber) and maintained by tracheal intubation (1.1%; 2–2.5 cc tidal volume; 60–70 strokes per minute). Rectal temperature was maintained at 37°C. A T12–L6 laminectomy was performed before fixing on a stereotaxic apparatus (Kopf Instruments, Tujunga, CA), and the exposed spinal cord was covered with warm (37°C) mineral oil.

Cells were isolated from L3–L5 medially near the dorsal root entry zone up to a depth of 1000 μm. Extracellular single-unit recordings were made with a low-impedance 5 MΩ tungsten insulated microelectrode (A-M Systems, Carlsburg, WA). Once a cell was identified, its receptive field was mapped and stimulated by an experimenter blinded to the surgical status of the animal and with the audio monitor silenced. Background activity was measured followed by cutaneous receptive field mapping with von Frey filaments or brief pinches, or both. Three routine mechanical stimuli were applied: (1) brush stimulation (BR) of the skin with a cotton brush; (2) pressure (PR), by attaching a large arterial clip with a weak grip to a fold of skin (144 gm/mm^2); and (3) pinch (PI), by applying a small arterial clip with a strong grip to a fold of skin (583 gm/mm^2). Next, increasing-intensity von Frey filaments (0.39, 1.01, 20.8 gm forces) and thermal stimuli (47°C steel probe, 1 cm^2 surface area) were applied. Multireceptive (MR) cells were identified by their responsiveness to BR, more so to PR and PI, and with increasing responses to incrementing strength von Frey stimuli. Background activity was recorded for 20 sec, and stimuli were applied serially for 20 sec, separated by another 20 sec of baseline activity. Care was taken to ensure that the responses were maximal, that each stimulus was applied to the primary receptive field of the cell, and that isolated units remained intact and held for the duration of each experiment using Spike2 template matching routines. Neurons responding chiefly to joint movement or to probing subcutaneous tissue were excluded from analysis. After SCI or ODN administration, or both, neurons were considered to be hyperexcitable if evoked responses were >150% of control levels for BR, PR, and PI stimuli.

Electrical signals were amplified and filtered at 300–3000 Hz (DAM80, World Precision Instruments, Sarasota, FL), processed by a data collection system (CED 1401+; Cambridge Instruments, Cambridge, UK), and stored on a computer (Pentium 4 PC, Dell, Austin, TX) to construct peristimulus time histograms or wavemark files. The stored digital record of individual unit activity was retrieved and analyzed off-line with Spike2 software (v3.13, Cambridge Electronic Design, Cambridge, UK). Evoked responses and afterdischarges were calculated by subtracting the prestimulus baseline activity to yield a net increase in discharge rate.

Statistical analysis. All statistical tests were performed at the α level of significance of 0.05 by two-tailed analyses using parametric tests. Data were tested for significance using one-way ANOVA to determine the degree of variability within a sample and whether there was a difference between groups among the obtained means, followed by Bonferroni *post hoc* analysis. Tests of factors were used including pair-wise comparisons where appropriate with either the paired Student's *t* test for before–after comparisons or the two sample Student's *t* test to compare two groups. Data management and statistical analyses were performed using SAS (1992) statistical procedures with Jandel SigmaStat (v1.0) and graphed using Jandel SigmaPlot (v7.0) as mean ± SD.

Table 1. Number of $Na_v1.3$-positive neuronal profiles and $Na_v1.3$ fluorescent signal intensity per section in lamina I–V neurons at L3–L5 segments in sham-operated animals and animals 4 weeks after T9 contusion SCI

	$Na_v1.3$ IF profiles		$Na_v1.3$ IF levels	
	Control	SCI	Control	SCI
Lamina I	5.2 ± 4.6	45.0 ± 6.2*	7.8 ± 2.6	49.2 ± 7.3*
Lamina II	3.4 ± 2.8	34.9 ± 4.3*	15.5 ± 6.8	66.1 ± 14.7*
Lamina III	3.9 ± 3.4	22.5 ± 5.0*	18.3 ± 8.5	62.0 ± 10.4*
Lamina IV	2.7 ± 2.4	24.4 ± 3.8*	20.0 ± 6.8	60.9 ± 7.6*
Lamina V	2.5 ± 1.9	20.6 ± 3.6*	17.2 ± 8.3	41.3 ± 9.3*

Data represent mean ± SD values [$n = 5$ sections per animal (10) per group]. *Significant difference from control group ($p < 0.05$). IF, Immunofluorescent.

Results

Behavioral testing

Using the BBB locomotor rating scale, open-field motor function was assessed after injury (Fig. 1*A*). Consistent with 25 mm contusion spinal cord injury (SCI), rats exhibited transient paraparesis and spontaneously recovered extensive movement of all three hindlimb joints with limb sweeping, plantar foot placement, and weight support in stance, achieving a mean ± SD. BBB score was 9.90 ± 1.51 at 28 d.

By 28 d after SCI, animals developed mechanical allodynia as demonstrated by decreases in paw withdrawal thresholds to von Frey stimulation (Fig. 1*B*). Mean ± SD mechanical thresholds

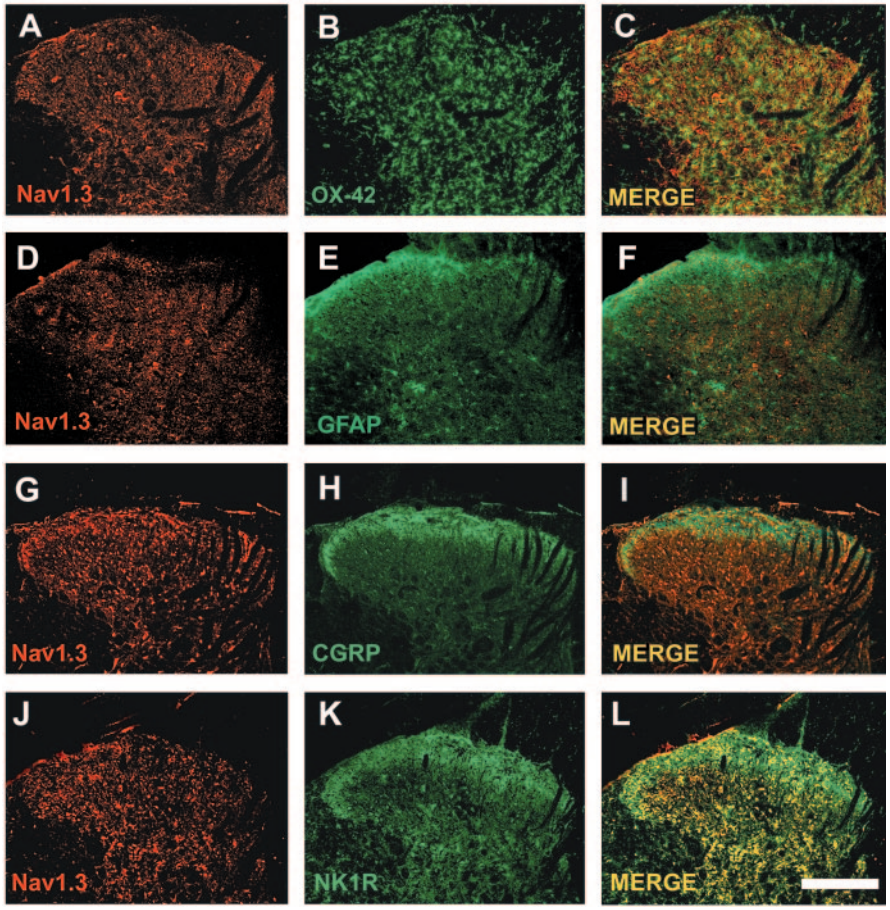

Figure 4. After SCI, colocalization experiments demonstrate that upregulation of $Na_v1.3$ took place in lumbar dorsal horn nociceptive neurons. $Na_v1.3$ (*A*) was not found to colocalize with OX-42 (*B*), a marker for microglia (*C*, merged image). Similarly, $Na_v1.3$ (*D*) was not found to colocalize with GFAP (*E*, *F*), a marker for astrocytes. $Na_v1.3$ (*G*) did not colocalize with CGRP (*H*, *I*), present within primary afferent terminals. Colocalization was observed between $Na_v1.3$ (*J*) and NK1R (*K*, *L*), which is present within second-order nociceptive neurons within laminas I–V. Colocalization was observed in neurons in superficial laminas I–II as well as in larger neurons in deeper laminas IV–V. Scale bar, 300 μm.

significantly decreased from 22.1 ± 3.03 gm before SCI to 4.05 ± 0.74 gm after SCI.

Thermal behavioral testing revealed that by 28 d after SCI, animals developed thermal hyperalgesia as indicated by decreases in paw withdrawal latency (Fig. 1*C*). Before SCI, the mean ± SD latency for all animals was 10.73 ± 0.79 sec. Twenty-eight days after SCI, latencies decreased significantly to 7.01 ± 0.94 sec.

In situ hybridization

In situ hybridization studies were performed on transverse lumbar spinal cord sections with a riboprobe specific for sodium channel $Na_v1.3$ mRNA (Fig. 2). These sections showed very little hybridization signal for $Na_v1.3$ in tissue collected from sham-operated animals (Fig. 2*A*). In contrast, extensive hybridization signal was observed in dorsal horn neuronal profiles after SCI (Fig. 2*B*). In sections in which signal was observed, labeling was mainly cytoplasmic and could be detected within small (5–10 μm) lamina I–II neurons, in addition to larger (20–40 μm) neurons deeper in lamina III–IV neurons. No labeling was observed in afferent fibers, or in dendritic or axonal arborizations. Very little signal was detected within white matter.

Compared with controls, the hybridization signal in neurons of the SCI group showed significantly increased intensity. Quantification of signal intensity revealed that $Na_v1.3$ in SCI sections was significantly increased to 63.63 ± 12.41 arbitrary units compared with 19.65 ± 6.39 in sham-operated controls. In addition, the number of strongly labeling neurons, defined by clear nuclear profile and strongly delineated boarders, per section in lamina I–IV neurons was significantly increased in SCI to 31.72 ± 3.89, compared with 3.04 ± 2.65 in sham-operated controls.

Quantitative RT-PCR

The change in $Na_v1.3$ mRNA amplification product collected from the lumbar enlargement of sham-operated and SCI groups is shown in Figure 2*C*. Quantitative RT-PCR results showed a statistically significant increase after SCI to ~125% of sham-operated $Na_v1.3$ mRNA levels.

Immunocytochemistry

Immunocytochemistry with an isoform-specific antibody raised against $Na_v1.3$ revealed light expression within the lumbar dorsal horn of sham-operated animals (Fig. 3*A*). Twenty-eight days after T9 spinal contusion injury, expression of $Na_v1.3$ was increased within the L3–L5 dorsal horn (Fig. 3*B*). Labeling was observed in smaller neurons within lamina I–II neurons as well as in deeper neurons in lamina III–V neurons. The spatial distribution of $Na_v1.3$ profiles from these sections is illustrated for controls (Fig. 3*C*) and SCI animals (Fig. 3*D*).

Quantification revealed that the mean number of immunofluorescent profiles was significantly increased in all laminas (I–V) after SCI (Table 1), from an average of 3.54 ± 3.02 profiles per lamina (average for lamina I–V neurons) in sham-operated controls to 29.48 ± 4.58 after SCI. In addition, immunofluorescent intensity was increased significantly in all laminas after SCI (Table 1), from an average for lamina I–V neurons of 15.76 ± 6.60 to 55.90 ± 9.86.

After SCI, colocalization experiments revealed that $Na_v1.3$ did not colocalize with OX-42, a marker for activated microglia, which was present in all laminas within the dorsal horn (Fig. 4*A–C*) or with GFAP, a marker for astrocytes, also localized to all spinal laminas (Fig. 4*D–F*), which both proliferate after SCI. CGRP, restricted to the terminals of primary afferent fibers within lamina I–II neurons, did not colocalize with $Na_v1.3$ protein (Fig. 4*G–I*). In contrast, NK1R, found in second-order nociceptive neurons within lamina I–IV neurons, was found to colocalize positively with $Na_v1.3$ (Fig. 4*J–L*).

Extracellular unit recordings

Representative peristimulus time histograms (spikes per 1 sec bin) are shown in Figure 5 for MR neurons in sham-operated (Fig. 5*A*) and SCI groups 28 d after injury (Fig. 5*B*). After SCI, spontaneous background activity rates of MR neurons were unchanged from sham-operated control rates. When compared with controls, SCI animals showed increased evoked activity to all natural peripheral stimuli (brush, press, pinch, 0.39 gm, 1.01 gm,

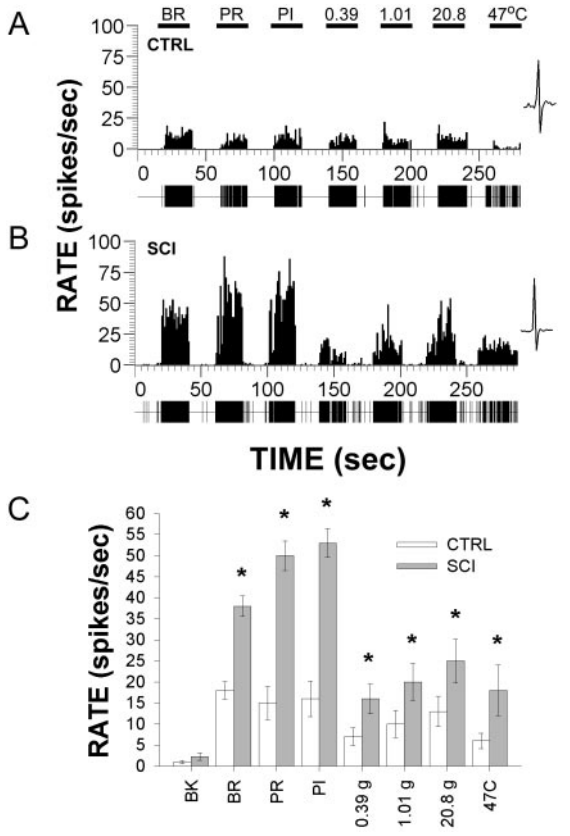

Figure 5. Representative peristimulus time histograms (spikes per 1 sec bin) of multireceptive neurons recorded extracellularly from L3–L5 in sham-operated control animals (*A*) and in animals 28 d after SCI (*B*) in response to various innocuous and noxious peripheral stimuli: brush (BR), press (PR), pinch (PI), increasing intensity von Frey filaments (0.39, 1.01, and 20.8 gm), and thermal (47°C). Single-unit waveforms are also shown to the right. Compared with controls, injured animals demonstrated evoked hyperexcitability to all peripheral stimuli. Spontaneous background activity was unchanged from control rates in injured animals. Quantification (*C*) of mean ± SD spontaneous and evoked discharge rates of neurons sampled from sham-operated controls ($n = 15$ cells) and SCI ($n = 15$ cells) groups demonstrated significantly (*$p < 0.05$) increased evoked activity to all peripheral stimuli after injury. No significant changes in background activity were detected.

20.81 gm von Frey filaments, and 47°C thermal stimuli). Of 18 MR cells sampled in SCI animals, 88% (16 of 18) were hyperexcitable.

Quantification of mean ± SD evoked discharge rates of MR cells, over background, from sham-operated and SCI groups is shown in Figure 5*C*. In comparison with sham-operated animals that demonstrated evoked response rates of up to 20 Hz to most stimuli, SCI animals demonstrated bilaterally increased response rates of up to 55–60 Hz. Responses were typical for MR cells, demonstrating high evoked activity to BR, PR, and PI stimuli and increasing rates to graded von Frey stimulation. Thermal responses were also increased in SCI animals, compared with sham-operated animals. All stimuli produced statistically significant increases in responsiveness, demonstrating evoked hyperexcitability (Fig. 5*C*).

ODN delivery

In the previous set of experiments, we have demonstrated that, after SCI, $Na_v1.3$ mRNA and protein are upregulated in dorsal horn sensory neurons. In the next set of experiments, we report the results of antisense knock-down experiments designed to decrease the contribution of $Na_v1.3$ to dorsal horn hyperexcitability and pain-related behaviors after SCI.

One-time intrathecal injection of AS oligodeoxynucleotides (45 μg/5 μl aCSF, followed by 10 μl of aCSF flush) labeled with Cy3 (to examine ODN penetration and uptake) resulted in readily observed pink staining of the dorsal surface of the spinal cord, extending for approximately three spinal segments (from L3 to L5) at 5 hr after injection when the animal was killed. Cross sections of spinal cord tissue from L3–L5 (Fig. 6*A*), observed at low magnification, show that Cy3 penetration was very strong within the spinal parenchyma to a depth of 400 μm below the dorsal surface of the cord and could still be detected to a depth of at least 800 μm below the dorsal surface, encompassing the territory of lamina I–IV neurons (Fig. 6*B*,*C*). Signal was noticeably stronger in gray matter and could be observed in individual cells exhibiting a neuronal morphology (Fig. 6*C*,*D*). High-magnification images (Fig. 6*D*′,*D*″) of two representative neurons at depths of ~500 and 800 μm show strong cytoplasmic uptake of Cy3-labeled AS. In these larger diameter neurons, Cy3 signal was also detected in their processes. Cy3 signal was not detectable in some cells, and signal intensity was variable in Cy3-positive cells, suggesting that not all cells were exposed to Cy3 after a single injection or that it was not taken up with equal efficacy.

Behavioral testing after ODN delivery

For testing the effects of ODN, on day 28, SCI animals were divided randomly into either AS or MM groups; before ODN administration, the groups were matched and did not differ significantly in terms of BBB scores, mechanical thresholds, or thermal paw withdrawal latencies. Pre-ODN BBB scores were 9.80 ± 0.84 and 9.41 ± 0.96 in SCI + MM and SCI + AS groups, respectively. Pre-ODN mechanical thresholds were 3.26 ± 1.99 and 3.99 ± 0.78 gm in SCI + MM and SCI + AS groups, respectively. Pre-ODN thermal latencies were 6.77 ± 1.00 and 6.9 ± 1.29 sec in SCI + MM and SCI + AS groups, respectively.

Four days after the start of AS or MM injections (day 34), BBB scores remained unchanged in all groups (Fig. 7*A*); scores were 10.14 ± 1.53, 9.90 ± 1.64, and 10.13 ± 1.46 for sham-operated, SCI + MM, and SCI + AS groups, respectively. Cessation of AS administration after 4 d had no effect on BBB scores, measured 5 d subsequently (9.96 ± 1.59). In naive animals (N + AS), AS administration had no effect on BBB scores, which remained at 21 throughout the course of the experiment (data not shown).

Administration of $Na_v1.3$ AS had a rapid and significant effect on mechanical thresholds and tended to reverse the decreases that occur with SCI (Fig. 7*B*). After 4 d of ODN injections, mechanical thresholds remained unchanged in SCI and SCI + MM groups: 3.01 ± 1.54 and 2.91 ± 1.64, respectively (Fig. 7*B*). In the SCI + AS group, paw withdrawal thresholds to von Frey stimulation increased to 14.36 ± 1.69 by day 4, representing a significant difference when compared with SCI and SCI + MM groups. Increases in thresholds were evident and statistically significant as soon as 1 d after the start of AS administration. Responses to a normally noxious pin prick stimuli remained unchanged (data not shown). After cessation of AS administration, mechanical thresholds returned to levels comparable with those before AS administration and MM levels (Fig. 7*B*). In naive animals (N + AS), AS administration had no effect on mechanical thresholds, which were not significantly different when measured before (21.78 ± 0.93) or after (20.35 ± 1.15) AS administration.

After SCI, animals receiving $Na_v1.3$ AS exhibited increased thermal paw withdrawal latencies. Four days after the start of

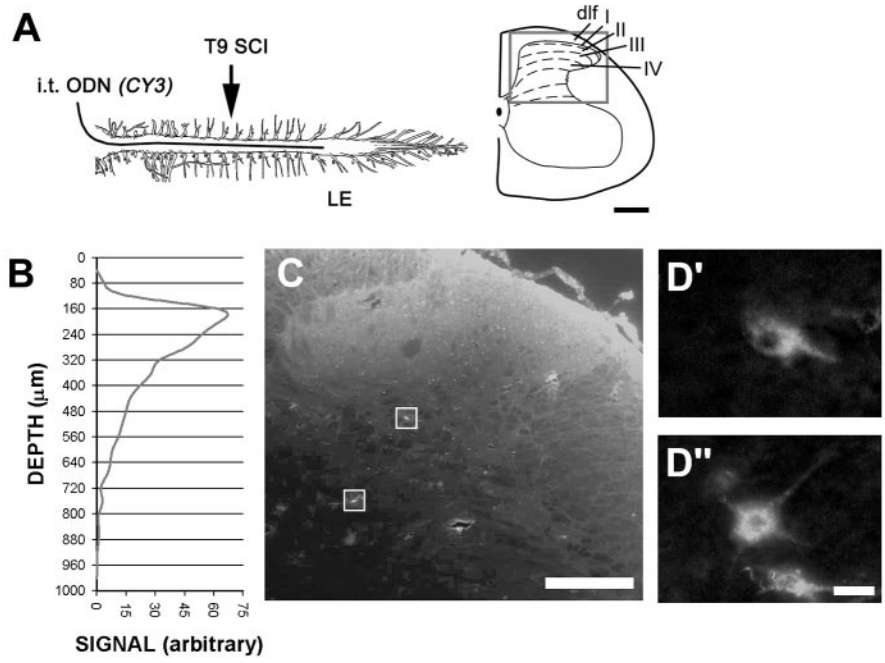

Figure 6. Schematic of injury and ODN delivery paradigm [i.t. ODN (CY3)] (*A*) showing relative locations of T9 contusion SCI, and intrathecally delivered AS or MM in relation to the lumbar enlargement (LE). A schematic cross section of the lumbar dorsal horn is shown illustrating field of view in *C*. After a one-time injection of Cy3-labeled AS (45 μg/5 μl of aCSF followed by 10 μl of aCSF flush), Cy3 fluorescence is detectable to a depth of 800 μm below the dorsal surface of the spinal cord (*B*) and can be seen to penetrate as far as lamina V (*C*). Higher-magnification image of cells exhibiting neuronal profiles (*C*, boxes) shows strong uptake of Cy3-labeled AS into cells with neuronal morphologies (*D'*, *D''*) after a single injection. Scale bar: *A*, *C*, 300 μm; *D'*, *D''*, 10 μm.

ODN injections, paw withdrawal latencies remained unchanged in SCI and SCI + MM groups: 8.41 ± 1.65 and 7.22 ± 1.12, respectively (Fig. 7*C*). In the SCI + AS group, paw withdrawal latencies increased to 12.71 ± 1.36 by day 4, representing a significant difference when compared with SCI and SCI + MM groups. Increases in latencies were evident (but not statistically significant) as soon as 1 d after the start of AS administration; the difference became significantly different by day 3 (Fig. 7*C*). After cessation of AS administration, latencies decreased to pre-AS levels (Fig. 7*C*). In naive animals (N + AS), AS administration had no effect on thermal thresholds, which were not significantly different when measured before (11.16 ± 1.07) or after (10.75 ± 0.80) AS administration.

ODN *in situ* hybridization

As in the SCI group, extensive *in situ* hybridization signal was observed in dorsal horn neurons 4 d after SCI + MM injections (Fig. 8*A*). Staining density and distribution were not noticeably different between SCI and SCI + MM groups. Signal intensity for $Na_v1.3$ was substantially reduced after 4 d of AS treatment of SCI animals (Fig. 8*B*). Quantification of $Na_v1.3$ signal intensity revealed that in SCI + AS sections, intensity was significantly decreased compared with SCI + MM sections: from 62.31 ± 10.73 to 30.34 ± 13.15 arbitrary units, respectively. The number of strongly labeled neurons, per section, in lamina I–IV neurons was significantly decreased after AS treatment to 15.28 ± 2.83 from 37.22 ± 3.65 in the SCI + MM group.

ODN quantitative RT-PCR

Quantitative RT-PCR results (Fig. 8*C*) showed a decrease in $Na_v1.3$ mRNA 4 d after AS injections compared with SCI + MM animals. This difference was statistically significant. $Na_v1.3$ levels in SCI + MM animals were elevated 133% relative to sham-operated control animals, whereas SCI + AS animals were increased 103% compared with controls.

ODN immunocytochemistry

Four days after ODN administration, SCI + AS animals demonstrated decreased $Na_v1.3$ labeling density and distribution (Fig. 9*B*), with most dramatic immunofluorescence decreases observed in superficial laminas. Some immunopositive profiles were evident within the neck of the dorsal horn at approximately lamina V that are putative neuronal profiles. $Na_v1.3$ labeling in SCI + MM (Fig. 9*A*) animals was not different from that observed in SCI animals (Fig. 3*B*). In AS withdrawal animals (SCI + AS/WD), $Na_v1.3$ expression reemerged after cessation of AS administration (Fig. 9*C*). $Na_v1.3$ expression was seen in smaller neurons within lamina I–II neurons, as well as in deeper neurons in lamina III–IV neurons. The spatial distribution of $Na_v1.3$ profiles from these sections is illustrated for SCI + MM (Fig. 9*D*), SCI + AS (Fig. 9*E*), and SCI + AS/WD animals (Fig. 9*F*).

In naive animals (N + AS), AS administration had no effect on the normal levels of expression of $Na_v1.3$ (data not shown).

Quantification revealed that the mean number of immunofluorescent profiles was significantly decreased in animals receiving AS compared with MM (Table 2), from 31.80 ± 3.82 (average for lamina I–V neurons) to 13.44 ± 3.64 per section. In SC + AS/WD animals, the mean number of profiles was increased to 28.20 ± 3.87. In addition, the average immunofluorescent intensity for lamina I–V neurons was significantly decreased in AS-treated animals (Table 2), down to 21.34 ± 7.06 from 59.92 ± 6.44. In contrast, in SCI + AS/WD animals, the mean number of immunofluorescent profiles was not different from SCI + MM animals, at 50.44 ± 6.82.

Effect of ODN on extracellular unit recordings

Representative peristimulus time histograms (spikes per 1 sec bin) are shown in Figure 10 for MR neurons sampled in animals from SCI + MM (Fig. 10*A*), SCI + AS (Fig. 10*B*), and SCI + AS/WD (Fig. 10*C*) groups. Four days after initiation of ODN injections, evoked activity was markedly decreased to all stimuli (brush, press, pinch, 0.39 gm, 1.01 gm, 20.81 gm force von Frey filaments, and 47°C thermal stimuli) in SCI + AS animals. Compared with SCI and SCI + MM, neurons from SCI + AS animals exhibited a reduced incidence of hyperexcitability. Of 19 MR cells sampled in the SCI + MM group, 89% were hyperexcitable (17 of 19), whereas of the 20 MR cells sampled in SCI + AS animals only 20% (4 of 20) were hyperexcitable. MM treatment had no apparent effect on evoked discharge rates of MR cells after SCI. In the SCI + MM group, neurons remained highly responsive to peripheral stimulation. In animals that had undergone SCI and AS administration, 5 d after cessation of AS administration (SCI + AS/WD) 90% of sampled cells were hyperexcitable (10 of 11) (Fig. 10*C*).

Quantification of mean ± SD discharge rates of MR cells, over background, from SCI + MM and SCI + AS groups is shown in

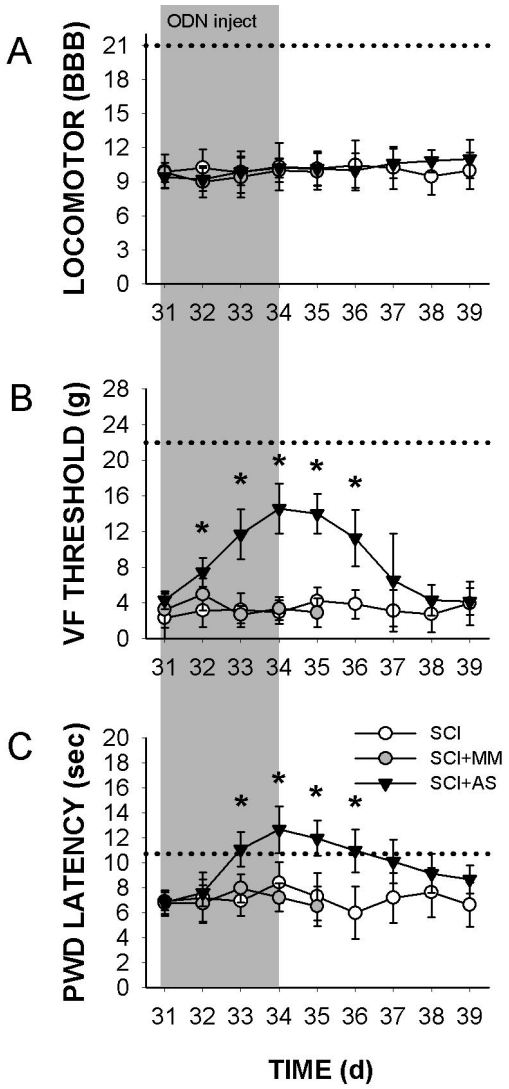

Figure 7. Behavioral changes after T9 spinal contusion injury and intrathecal administration (days 31–34, shaded) of either MM or AS sequences generated against $Na_v1.3$ ($n = 10$ animals per group, except for SC + AS/WD where $n = 6$). The dotted line in each panel indicates sham-operated control thresholds. Mean ± SD. BBB open-field locomotor scores (*A*) did not change during the course of ODN administration or after cessation of ODN injections, in any groups. One day after initiation of ODN administration, mean ± SD von Frey mechanical (VF) thresholds (*B*) began to increase in AS-treated animals, eventually rising to 18 gm by day 4. A significant ($*p < 0.05$) difference when compared with SCI and SCI–MM groups. Cessation of AS administration resulted in restoration of mechanical allodynia. By 2 d of ODN administration, mean ± SD paw withdrawal (PWD) latency (*C*) to radiant thermal stimuli increased significantly ($*p < 0.05$) in AS-treated animals, compared with SCI and SCI + MM groups. In these ODN-treated animals, latencies were not significantly different from sham-operated control latencies. Cessation of AS administration resulted in restoration of thermal hyperalgesia.

Figure 10*D*. Animals receiving AS injections demonstrated significantly decreased evoked discharge rates to all peripheral stimuli compared with SCI + MM animals. Firing rates were proportionally decreased in response to graded mechanical stimuli, such as von Frey filaments, of increasing intensity. Evoked discharge rates in SCI + AS animals were not significantly different from the evoked rates in the sham-operated animals except for pinch stimulus. Evoked discharge rates of cells from SCI + AS/WD animals were significantly increased compared with SCI + AS animals and not significantly different from SCI + MM animals.

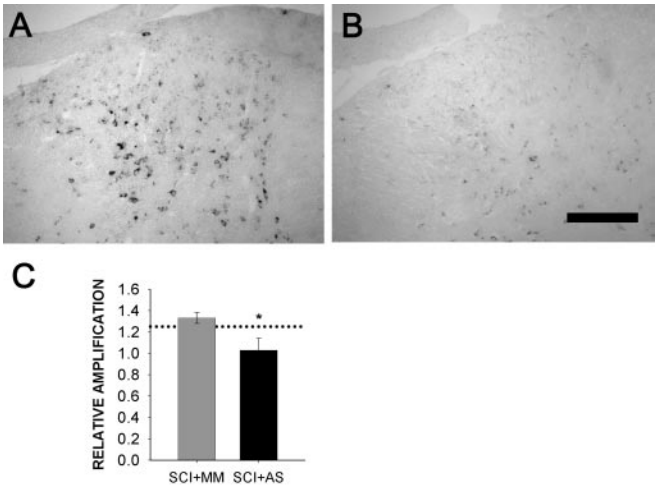

Figure 8. *In situ* hybridization for $Na_v1.3$ after SCI and administration of MM or AS sequences generated against $Na_v1.3$. In animals treated with MM for 4 d (*A*), widely distributed punctate staining was observed throughout the lumbar dorsal horn in small and large cells exhibiting neuronal morphologies, similar to untreated SCI (Fig. 2*B*). In contrast, in AS-treated animals (*B*), $Na_v1.3$ hybridization signal was markedly decreased in both intensity and distribution throughout the lumbar dorsal horn. Quantitative RT-PCR amplification (*C*) showed a significant ($*p < 0.05$) decrease in lumbar $Na_v1.3$ mRNA in the SCI + AS group ($n = 10$ animals) when compared with SCI + MM animals ($n = 10$). Dotted line indicates mRNA levels in SCI group. Scale bar, 300 μm.

Discussion

In the present study, we examined changes in the expression of $Na_v1.3$ within the lumbar dorsal horn after thoracic contusion SCI and used targeted AS knock-down techniques to assess the functional contribution of $Na_v1.3$ to hyperexcitability of dorsal horn sensory neurons and central neuropathic pain that develops after SCI. The present data confirm that after SCI animals develop mechanical allodynia and thermal hyperalgesia and that dorsal horn neurons exhibit increased evoked responsiveness to peripheral stimulation. We show for the first time that after SCI (1) $Na_v1.3$ mRNA and protein are upregulated in lumbar dorsal horn nociceptive neurons, (2) targeted AS knock-down of $Na_v1.3$ causes a downregulation of $Na_v1.3$ mRNA and protein, and (3) AS knock-down of $Na_v1.3$ confers a reduction in hyperexcitability of dorsal horn sensory neurons and pain-related behaviors.

Antisense approaches have been used previously to examine the contribution of sodium channels to peripheral neuropathic pain. Using this paradigm, it has been demonstrated that $Na_v1.8$ contributes to increased tetrodotoxin-resistant (TTX-R) I_{Na} current density and hyperalgesia after prostaglandin E_2-induced peripheral inflammation (Khasar et al., 1998). Similarly, $Na_v1.8$ has been associated with visceral pain (Yoshimura et al., 2001) and neuropathic pain after spinal nerve ligation (Lai et al., 2002; Gold et al., 2003) using AS knock-down strategies. As yet, the contribution of $Na_v1.3$ to central neuropathic pain has not yet been examined using AS or other methods.

Upregulated expression of $Na_v1.3$ in dorsal horn neurons after SCI

Our results include several novel findings. First, we report that upregulated expression of $Na_v1.3$ occurs within sensory neurons of the spinal dorsal horn as a result of trauma to the CNS. Earlier studies showed that $Na_v1.3$ expression is detectable at embryonic day 17 in spinal cord neurons but is downregulated with further development and exhibits very low levels of expression by P30

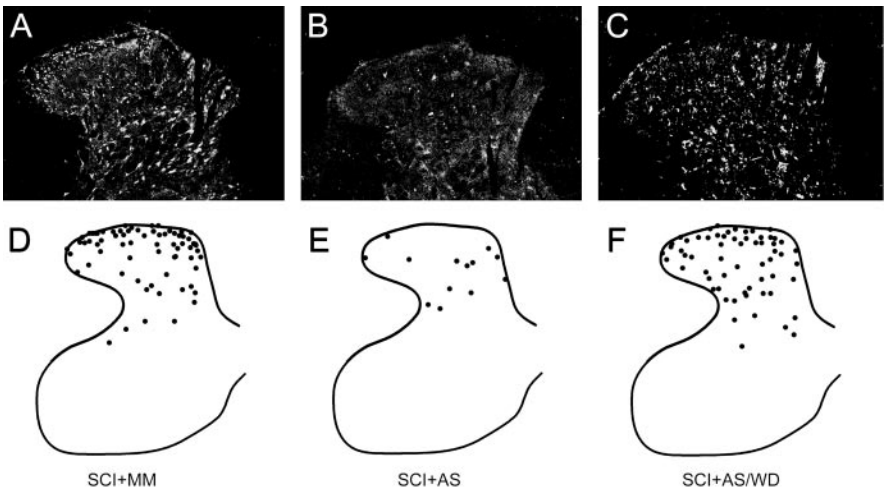

Figure 9. Immunocytochemical localization of $Na_v1.3$ protein within lumbar dorsal horn in SCI animals after administration of MM or AS sequences against $Na_v1.3$. In animals that received MM injections (*A*), $Na_v1.3$-immunopositive cell profiles were widely distributed throughout the lumbar dorsal horn, similar to untreated SCI (Fig. 3*B*). These neurons were of both small and large diameter. In contrast, in animals receiving AS injections (*B*), the number of immunopositive cell profiles was markedly decreased within the dorsal horn. A decrease in distribution was most notable in lamina I–III neurons. After cessation of AS administration, (*C*), the number $Na_v1.3$-immunopositive cell profiles was increased. Localization of immunopositive profiles from a number of sections ($n = 4$) plotted on a representative schematic of the lumbar spinal cord (*D–F*) shows that in AS-treated animals, but not after interruption of AS administration, the number of profiles was decreased within all laminas. Scale bar, 300 μm.

(Beckh et al., 1989; Felts et al., 1997). In this paper, we document the upregulation of $Na_v1.3$ after SCI, specifically in second-order nociceptive neurons, and not in afferent fibers, astrocytes, or microglia, which are known to proliferate after SCI.

Very few studies have examined changes in sodium channel expression in spinal cord or DRG neurons after SCI. Spinal transection results in a shift from high-threshold TTX-R- to low-threshold TTX-S-type sodium channel populations in bladder afferent DRG neurons (Yoshimura and de Groat, 1997), partly through decreased expression of $Na_v1.8$ (Black et al., 2003). After spinal cord contusion, hints of changes in expression of sodium channel genes are suggested by oligonucleotide-based microarray analysis. Song et al. (2001) reported that at the lesion epicenter, $Na_v1.1$ mRNA is decreased as soon as 3 hr after impact. Carmel et al. (2001) (http://spine.rutgers.edu/microarray) reported that $Na_v1.3$ mRNA is slightly decreased at the injury site and 5 mm caudal to the epicenter, 48 hr after injury.

Increased $Na_v1.3$ mRNA and protein expression occur in DRG neurons after both transection (Waxman et al., 1994; Dib-Hajj et al., 1996; Black et al., 1999) and tight ligation (Kim et al., 2001) of the sciatic nerve and in facial motor neurons after transection of the facial nerve (Iwahashi et al., 1994). Several studies have indicated that the newly synthesized $Na_v1.3$ channels within these axotomized neurons produce a rapidly repriming sodium current that appears to contribute to hyperexcitability (Cummins and Waxman, 1997; Black et al., 1999). Similar changes in DRG sodium channel gene activity have been seen in the chronic constriction nerve injury model, in association with allodynia and hyperalgesia (Dib-Hajj et al., 1999).

$Na_v1.3$ contributes to hyperexcitability of dorsal horn neurons after SCI

A second novel finding is that $Na_v1.3$ functionally contributes to the hyperexcitability of dorsal horn sensory neurons after SCI. Most previous studies on sodium channels and neuropathic pain have focused on changes in channel expression within primary sensory (DRG) neurons after injury to their peripheral axons (Devor, 1994; McCleskey and Gold, 1999; Porreca et al., 1999); however, consistent with a role of sodium channels in hyperexcitability of dorsal horn neurons, ionophoretic application of the sodium channel blockers lamotrigine and flunarizine markedly decreases high-threshold responsiveness (Blackburn-Munro and Fleetwood-Walker, 1997). Similarly, spinally administered bupivacaine reduces C-fiber-evoked responses, wind up, and afterdischarge activity of dorsal horn neurons (Chapman et al., 1997). Together with these earlier studies, our results establish a link between sodium channel activity and hyperexcitability of dorsal horn neurons associated with neuropathic pain.

With selective knock-down of $Na_v1.3$, we were able to achieve a near-complete attenuation of the increased evoked activity of multireceptive cells associated with SCI. We did not discern, however, any effect of $Na_v1.3$ AS on nociceptive thresholds in normal animals, implicating upregulation of $Na_v1.3$ after SCI as a significant contributor to hyperexcitability. Consistent with this conclusion, *in vitro* experiments show that in DRG neurons, $Na_v1.3$ expression may confer an ability to fire repetitively at relatively high frequencies as a result of a rapid recovery from inactivation and slow closed-state inactivation kinetics (Cummins et al., 2001). After cessation of AS administration, $Na_v1.3$ protein, dorsal horn neuronal hyperexcitability, and pain-related behaviors all returned. By 5 d after AS cessation, $Na_v1.3$ protein levels, hyperexcitability, and pain-related behaviors were equivalent to levels measured before the initiation of AS administration after SCI and in SCI + MM animals. These observations further strengthen the association between $Na_v1.3$ and chronic neuropathic pain after SCI. The reemergence of $Na_v1.3$ expression suggests that the induction of $Na_v1.3$ is not caused by a transient event that occurs, for example, at the time of SCI, but that $Na_v1.3$ expression is induced and maintained by pathophysiologic consequences of SCI that persist for at least 34 d.

Whether changes in $Na_v1.3$ expression after SCI are exclusively responsible for hyperexcitability of dorsal horn neurons is unknown. Multiple subtypes of sodium channels are expressed by a single neuron, and the relative contribution of $Na_v1.3$ or other channels remains untested. Spinal neurons also express detectable levels of $Na_v1.1$, $Na_v1.2$, and $Na_v1.6$ (Felts et al., 1997; Krzemien et al., 2000). Although BLAST search revealed no sequence homology between our $Na_v1.3$ antisense construct and any of these channels, we cannot exclude the possibility of a secondary change in expression of one or more of these channels after knock-down of $Na_v1.3$ or exclude a nonspecific effect on other types of channels. It is possible that changes in the expression of these (or other) ion channels could contribute to changes in threshold, refractory period, or the ability to generate and conduct high-frequency trains of action potentials after SCI (Schild and Kunze, 1997; Waxman, 2000). Furthermore, we cannot rule out the possibility that after SCI, transcriptional changes in $Na_v1.3$ and other channels may take place within the DRG neurons, which could result in increased input to spinal sensory neurons.

At this point, it is not known what mechanisms related to SCI

Table 2. Number of $Na_v1.3$-positive neuronal profiles and $Na_v1.3$ fluorescent signal intensity per section in lamina I–V neurons at L3–L5 segments in SCI animals after MM, AS, or AS withdrawal

	$Na_v1.3$ IF profiles			$Na_v1.3$ IF levels		
	SCI + MM	SCI + AS	SCI + AS/WD	SCI + MM	SCI + AS	SCI + AS/WD
Lamina I	49.2 ± 3.6	16.1 ± 4.5*	34.6 ± 6.4$^+$	61.5 ± 12.0	11.8 ± 7.2*	54.2 ± 9.4$^+$
Lamina II	40.2 ± 4.8	10.5 ± 2.6*	36.0 ± 2.6$^+$	66.4 ± 4.4	25.8 ± 9.6*	48.1 ± 6.6$^+$
Lamina III	25.7 ± 3.6	12.6 ± 2.7*	26.6 ± 4.1$^+$	65.6 ± 5.0	21.4 ± 5.7*	57.8 ± 8.7$^+$
Lamina IV	21.1 ± 4.2	15.6 ± 3.9*	21.6 ± 3.5$^+$	59.1 ± 7.6	21.6 ± 7.3*	52.5 ± 4.0$^+$
Lamina V	22.8 ± 2.9	12.4 ± 4.5*	22.0 ± 2.6$^+$	47.0 ± 3.2	26.1 ± 5.5*	39.6 ± 5.4$^+$

Data represent mean ± SD values [$n = 5$ sections per animal (10) per group]. *Significant difference from SCI + MM group ($p < 0.05$); $^+$significant difference from SCI + AS group ($p < 0.05$). IF, Immunofluorescent.

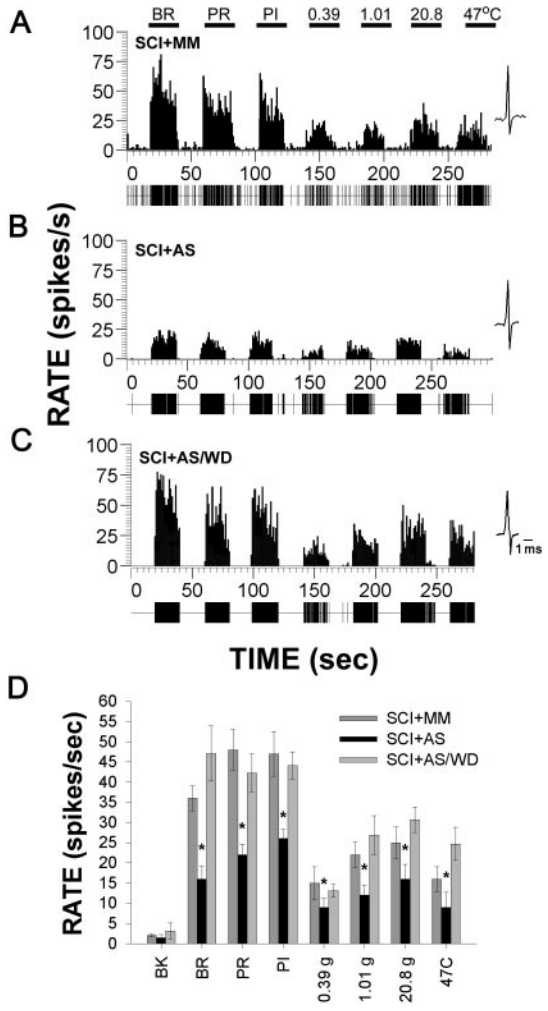

Figure 10. Representative peristimulus time histograms (spikes per 1 sec bin) of multireceptive neurons recorded extracellularly from L3–L5 in animals after administration of MM (*A*) or AS (*B*) sequences generated against $Na_v1.3$ after SCI. Records show evoked activity in response to various innocuous and noxious peripheral stimuli: brush (BR), press (PR), pinch (PI), increasing intensity von Frey filaments (0.39, 1.01, and 20.8 gm), and thermal (47°C). Single-unit waveforms are also shown. In MM-receiving animals (*A*), evoked hyperexcitability was demonstrated in response to all peripherally applied stimuli. In contrast, in animals receiving AS injections (*B*), evoked activity was decreased to all stimuli except PI. In a separate group of SCI + AS animals 5 d after cessation of AS administration (SCI + AS/WD) (*C*), cells were hyperexcitable. Spontaneous background activity was not significantly different in either group. Quantification (*D*) of mean ± SD spontaneous and evoked discharge rates of neurons sampled from MM- or AS-receiving animals ($n = 11$–15 cells sampled per group) demonstrated significantly (*$p < 0.05$) reduced evoked activity in AS-receiving animals only.

might contribute to the upregulation of $Na_v1.3$. One possibility is the influence of fluctuating levels of trophic factors. After peripheral nerve injury, levels of nerve growth factor (NGF) (Korsching et al., 1985; Nagata et al., 1987; Zhou et al., 1994) and its high-affinity TrkA receptor (Li et al., 2000) are decreased in DRG neurons, presumably because of interrupted peripheral transport. A link between NGF and sodium channels has been demonstrated *in vitro* (Rudy et al., 1987; Mandel et al., 1988; Kalman et al., 1990; Aguayo and White, 1992; Black et al., 1997) and *in vivo* (Dib-Hajj et al., 1998; Fjell et al., 1999). In an *in vitro* model of axotomy, it has been shown that exogenously added NGF prevents the upregulation of $Na_v1.3$ within DRG neurons (Black et al., 1997). In addition to NGF, intrathecally administered glial cell line-derived neurotrophic factor (GDNF) can reverse axotomy-induced expression of TTX-S current in DRG neurons (Leffler et al., 2002) and can reverse spontaneous activity, pain-related behaviors, and upregulation of $Na_v1.3$ after partial sciatic ligation and L5 spinal nerve ligation (Boucher et al., 2000).

After T13 hemisection injury, it is reported that NGF levels decrease at L2 by two- to fourfold until 7 d after injury within the spinal cord (Bennett et al., 1999). Others show that NGF levels increase by three- to fourfold at the site of a mid-thoracic over-hemisection (Nakamura and Bregman, 2001) or contusion (Widenfalk et al., 2001) injury. After contusion SCI, TrkA expression is decreased surrounding the lesion site, but beyond that levels were unchanged (Liebl et al., 2001). Additionally, GDNF has been shown to increase at the site of over-hemisection (Nakamura and Bregman, 2001) and contusion SCI (Satake et al., 2000; Widenfalk et al., 2001). Considering the ability of these factors to modulate $Na_v1.3$ expression (Black et al., 1997; Leffler et al., 2002), future studies on NGF and GDNF levels within injured spinal cord might prove to be informative.

In conclusion, the data presented here document the upregulated expression of the $Na_v1.3$ sodium channel in second-order nociceptive neurons within the lumbar enlargement after thoracic contusion SCI and demonstrate that knock-down of $Na_v1.3$ reduces hyperexcitability and attenuates mechanical allodynia and thermal hyperalgesia after experimental SCI. Together with previous work showing an association between $Na_v1.3$ and accelerated repriming of TTX-S sodium currents in injured DRG neurons (Cummins et al., 2001), our results suggest a functional link between upregulated expression of $Na_v1.3$ and hyperexcitability of dorsal horn sensory neurons associated with pain after SCI. Future studies will be needed to examine the molecular mechanisms responsible for the upregulation of $Na_v1.3$ and to ascertain whether there are changes in the expression of other channels.

References

Aguayo LG, White G (1992) Effects of nerve growth factor on TTX- and capsaicin-sensitivity in adult rat sensory neurons. Brain Res 570:61–67.

Balazy TE (1992) Clinical management of chronic pain in spinal cord injury. Clin J Pain 8:102–110.

Basso M, Beattie MS, Bresnahan JC (1995) A sensitive and reliable locomotor rating scale for open field testing in rats. J Neurotrauma 12:1–21.

Beckh S, Noda M, Lubbert H, Numa S (1989) Differential regulation of three sodium channel messenger RNAs in the rat central nervous system during development. EMBO J 8:3611–3616.

Bennett AD, Taglialatela G, Perez-Polo R, Hulsebosch CE (1999) NGF levels decrease in the spinal cord and dorsal root ganglion after spinal hemisection. NeuroReport 10:889–893.

Black JA, Dib-Hajj S, McNabola K, Jeste S, Rizzo MA, Kocsis JD, Waxman SG (1996) Spinal sensory neurons express multiple sodium channel alpha-subunit mRNAs. Mol Brain Res 43:117–131.

Black JA, Langworthy K, Hinson AW, Dib-Hajj SD, Waxman SG (1997) NGF has opposing effects on Na^+ channel III and SNS gene expression in spinal sensory neurons. NeuroReport 8:2331–2335.

Black JA, Cummins TR, Plumpton C, Chen YH, Hormuzdiar W, Clare JJ, Waxman SG (1999) Upregulation of a silent sodium channel after peripheral, but not central, nerve injury in DRG neurons. J Neurophysiol 82:2776–2785.

Black JA, Cummins TR, Yoshimura N, de Groat WC, Waxman SG (2003) Tetrodotoxin-resistant sodium channels Nav1.8/SNS and Nav1.9/NaN in afferent neurons innervating urinary bladder in control and spinal cord injured rats. Brain Res 963:132–138.

Blackburn-Munro G, Fleetwood-Walker SM (1997) The effects of Na^+ channel blockers on somatosensory processing by rat dorsal horn neurones. NeuroReport 8:1549–1554.

Boucher TJ, Okuse K, Bennett DL, Munson JB, Wood JN, McMahon SB (2000) Potent analgesic effects of GDNF in neuropathic pain states. Science 290:124–127.

Brysch W, Creutzfeldt OD, Luno K, Schlingensiepen R, Schlingensiepen KH (1991) Regional and temporal expression of sodium channel messenger RNAs in the rat brain during development. Exp Brain Res 86:562–567.

Carmel JB, Galante A, Soteropoulos P, Tolias P, Recce M, Young W, Hart RP (2001) Gene expression profiling of acute spinal cord injury reveals spreading inflammatory signals and neuron loss. Physiol Genomics 7:201–213.

Chaplan SR, Bach FW, Pogrel JW, Chung JM, Yaksh TL (1994) Quantitative assessment of tactile allodynia in the rat paw. J Neurosci Methods 53:55–63.

Chapman V, Wildman MA, Dickenson AH (1997) Distinct electrophysiological effects of two spinally administered membrane stabilising drugs, bupivacaine and lamotrigine. Pain 71:285–295.

Cummins TR, Waxman SG (1997) Downregulation of tetrodotoxin-resistant sodium currents and upregulation of a rapidly repriming tetrodotoxin-sensitive sodium current in small spinal sensory neurons following nerve injury. J Neurosci 17:3503–3514.

Cummins TR, Aglieco F, Renganathan M, Herzog RI, Dib-Hajj SD, Waxman SG (2001) Nav1.3 sodium channels: rapid repriming and slow closed-state inactivation display quantitative differences after expression in a mammalian cell line and in spinal sensory neurons. J Neurosci 21:5952–5961.

Devor M (1994) The pathophysiology of damaged peripheral nerves. In: Textbook of pain, Ed 2 (Wall PD, Melzack R, eds), pp 79–101. Edinburgh: Churchill Livingstone.

Dib-Hajj S, Black JA, Felts P, Waxman SG (1996) Down-regulation of transcripts for Na channel-SNS in spinal sensory neurons following axotomy. Proc Natl Acad Sci USA 93:14950–14954.

Dib-Hajj SD, Black JA, Cummins TR, Kenney AM, Kocsis JD, Waxman SG (1998) Rescue of alpha-SNS sodium channel expression in small dorsal root ganglion neurons after axotomy by nerve growth factor in vivo. J Neurophysiol 79:2668–2676.

Dib-Hajj SD, Fjell J, Cummins TR, Zheng Z, Fried K, LaMotte R, Black JA, Waxman SG (1999) Plasticity of sodium channel expression in DRG neurons in the chronic constriction model of neuropathic pain. Pain 83:591–600.

Dirig DM, Salami A, Rathbun ML, Ozaki GT, Yaksh TL (1997) Characterization of variables defining hindpaw withdrawal latency evoked by radiant thermal stimuli. J Neurosci Methods 76:183–191.

Dixon WJ (1980) Efficient analysis of experimental observations. Annu Rev Pharmacol Toxicol 20:441–462.

Drew GM, Siddall PJ, Duggan AW (2001) Responses of spinal neurones to cutaneous and dorsal root stimuli in rats with mechanical allodynia after contusive spinal cord injury. Brain Res 893:59–69.

Felts PA, Yokoyama S, Dib-Hajj S, Black JA, Waxman SG (1997) Sodium channel alpha-subunit mRNAs I, II, III, NaG, Na6 and hNE (PN1): different expression patterns in developing rat nervous system. Mol Brain Res 45:71–82.

Fjell J, Cummins TR, Dib-Hajj SD, Fried K, Black JA, Waxman SG (1999) Differential role of GDNF and NGF in the maintenance of two TTX-resistant sodium channels in adult DRG neurons. Mol Brain Res 67:267–282.

Furuyama T, Morita Y, Inagaki S, Takagi H (1993) Distribution of I, II and III subtypes of voltage-sensitive Na^+ channel mRNA in the rat brain. Mol Brain Res 17:169–173.

Gold MS, Weinreich D, Kim CS, Wang R, Treanor J, Porreca F, Lai J (2003) Redistribution of Na(V)1.8 in uninjured axons enables neuropathic pain. J Neurosci 23:158–166.

Gruner JA (1992) A monitored contusion model of spinal cord injury in the rat. J Neurotrauma 9:123–126.

Hains BC, Yucra JA, Hulsebosch CE (2001) Selective COX-2 inhibition with NS-398 preserves spinal parenchyma and attenuates behavioral deficits following spinal contusion injury. J Neurotrauma 18:409–423.

Hains BC, Black JA, Waxman SG (2002) Primary motor neurons fail to up-regulate voltage-gated sodium channel Na(v)1.3/brain type III following axotomy resulting from spinal cord injury. J Neurosci Res 70:546–552.

Hains BC, Eaton MJ, Willis WD, Hulsebosch CE (2003a) Engraftment of serotonergic precursors amends hyperexcitability of dorsal horn neurons after spinal hemisection-induced central sensitization. Neuroscience 116:1097–1110.

Hains BC, Willis WD, Hulsebosch CE (2003b) Temporal plasticity of dorsal horn somatosensory neurons after acute and chronic spinal cord hemisection in rat. Brain Res 970:238–241.

Hao JX, Xu XJ, Aldskogius H, Seiger A, Wiesenfeld-Hallin Z (1991) Allodynia-like effects in rat after ischaemic spinal cord injury photochemically induced by laser irradiation. Pain 45:175–185.

Huang PP, Young W (1994) The effects of arterial blood gas values on lesion volumes in a graded rat spinal cord contusion model. J Neurotrauma 11:547–562.

Hulsebosch CE, Xu GY, Perez-Polo JR, Westlund KN, Taylor CP, McAdoo DJ (2000) Rodent model of chronic central pain after spinal cord contusion injury and effects of gabapentin. J Neurotrauma 17:1205–1217.

Iwahashi Y, Furuyama T, Inagaki S, Morita Y, Takagi H (1994) Distinct regulation of sodium channel types I, II and III following nerve transection. Mol Brain Res 22:341–345.

Kalman D, Wong B, Horvai AE, Cline MJ, O'Lague PH (1990) Nerve growth factor acts through cAMP-dependent protein kinase to increase the number of sodium channels in PC12 cells. Neuron 4:355–366.

Khasar SG, Gold MS, Levine JD (1998) A tetrodotoxin-resistant sodium current mediates inflammatory pain in the rat. Neurosci Lett 256:17–20.

Kim CH, Oh Y, Chung JM, Chung K (2001) The changes in expression of three subtypes of TTX sensitive sodium channels in sensory neurons after spinal nerve ligation. Mol Brain Res 95:153–161.

Korsching S, Auburger G, Heumann R, Scott J, Thoenen H (1985) Levels of nerve growth factor and its mRNA in the central nervous system of the rat correlate with cholinergic innervation. EMBO J 4:1389–1393.

Krzemien DM, Schaller KL, Levinson SR, Caldwell JH (2000) Immunolocalization of sodium channel isoform NaCh6 in the nervous system. J Comp Neurol 420:70–83.

Lai J, Gold MS, Kim CS, Bian D, Ossipov MH, Hunter JC, Porreca F (2002) Inhibition of neuropathic pain by decreased expression of the tetrodotoxin-resistant sodium channel, NaV1.8. Pain 95:143–152.

Leffler A, Cummins TR, Dib-Hajj SD, Hormuzdiar WN, Black JA, Waxman SG (2002) GDNF and NGF reverse changes in repriming of TTX-sensitive Na(+) currents following axotomy of dorsal root ganglion neurons. J Neurophysiol 88:650–658.

Li L, Deng YS, Zhou XF (2000) Downregulation of TrkA expression in primary sensory neurons after unilateral lumbar spinal nerve transection and some rescuing effects of nerve growth factor infusion. Neurosci Res 38:183–191.

Liebl DJ, Huang W, Young W, Parada LF (2001) Regulation of Trk receptors following contusion of the rat spinal cord. Exp Neurol 167:15–26.

Lindsey AE, LoVerso RL, Tovar CA, Hill CE, Beattie MS, Bresnahan JC (2000) An analysis of changes in sensory thresholds to mild tactile and cold stimuli after experimental spinal cord injury in the rat. Neurorehabil Neural Repair 14:287–300.

Mandel G, Cooperman SS, Maue RA, Goodman RH, Brehm P (1988) Selective induction of brain type II Na+ channels by nerve growth factor. Proc Natl Acad Sci USA 85:924–928.

Matzner O, Devor M (1992) Na+ conductance and the threshold for repetitive neuronal firing. Brain Res 597:92–98.

McCleskey EW, Gold MS (1999) Ion channels of nociception. Annu Rev Physiol 61:835–856.

Mills CD, Hains BC, Johnson KM, Hulsebosch CE (2001) Strain and model dependence of locomotor deficits and development of chronic central pain after spinal cord injury. J Neurotrauma 18:743–756.

Nagata Y, Ando M, Takahama K, Iwata M, Hori S, Kato K (1987) Retrograde transport of endogenous nerve growth factor in superior cervical ganglion of adult rats. J Neurochem 49:296–302.

Nakamura M, Bregman BS (2001) Differences in neurotrophic factor gene expression profiles between neonate and adult rat spinal cord after injury. Exp Neurol 169:407–415.

Porreca F, Lai J, Bian D, Wegert S, Ossipov MH, Eglen RM, Kassotakis L, Novakovic S, Rabert DK, Sangameswaran L, Hunter JC (1999) A comparison of the potential role of the tetrodotoxin-insensitive sodium channels, PN3/SNS and NaN/SNS2, in rat models of chronic pain. Proc Natl Acad Sci USA 96:7640–7644.

Rudy B, Kirschenbaum B, Rukenstein A, Greene LA (1987) Nerve growth factor increases the number of functional Na channels and induces TTX-resistant Na channels in PC12 pheochromocytoma cells. J Neurosci 7:1613–1625.

Satake K, Matsuyama Y, Kamiya M, Kawakami H, Iwata H, Adachi K, Kiuchi K (2000) Up-regulation of glial cell line-derived neurotrophic factor (GDNF) following traumatic spinal cord injury. NeuroReport 11:3877–3881.

Schild JH, Kunze DL (1997) Experimental and modeling study of Na+ current heterogeneity in rat nodose neurons and its impact on neuronal discharge. J Neurophysiol 78:3198–3209.

Song G, Cechvala C, Resnick DK, Dempsey RJ, Rao VL (2001) GeneChip analysis after acute spinal cord injury in rat. J Neurochem 79:804–815.

Turner JA, Cardenas DD, Warms CA, McClellan CB (2001) Chronic pain associated with spinal cord injuries: a community survey. Arch Phys Med Rehabil 82:501–509.

Vincler M, Maixner W, Vierck CJ, Light AR (2001) Effects of systemic morphine on escape latency and a hindlimb reflex response in rat. J Pain 2:83–90.

Waxman SG (2000) The neuron as a dynamic electrogenic machine: modulation of sodium channel expression as a basis for functional plasticity in neurons. Philos Trans R Soc Lond B Biol Sci 355:199–213.

Waxman SG, Kocsis JD, Black JA (1994) Type III sodium channel mRNA is expressed in embryonic but not adult spinal sensory neurons, and is re-expressed following axotomy. J Neurophysiol 72:466–471.

Waxman SG, Dib–Hajj SD, Cummins TR, Black JA (1999) Sodium channels and pain. Proc Natl Acad Sci USA 96:7635–7639.

Widenfalk J, Lundstromer K, Jubran M, Brene S, Olson L (2001) Neurotrophic factors and receptors in the immature and adult spinal cord after mechanical injury or kainic acid. J Neurosci 21:3457–3475.

Winer J, Jung CK, Shackel I, Williams PM (1999) Development and validation of real-time quantitative reverse transcriptase-polymerase chain reaction for monitoring gene expression in cardiac myocytes in vitro. Anal Biochem 270:41–49.

Woolf CJ (1984) Long term alterations in the excitability of the flexion reflex produced by peripheral tissue injury in the chronic decerebrate rat. Pain 18:325–343.

Yezierski RP, Park SH (1993) The mechanosensitivity of spinal sensory neurons following intraspinal injections of quisqualic acid in the rat. Neurosci Lett 157:115–119.

Yoshimura N, de Groat WC (1997) Plasticity of Na+ channels in afferent neurones innervating rat urinary bladder following spinal cord injury. J Physiol (Lond) 503:269–276.

Yoshimura N, Seki S, Novakovic SD, Tzoumaka E, Erickson VL, Erickson KA, Chancellor MB, de Groat WC (2001) The involvement of the tetrodotoxin-resistant sodium channel Na(v)1.8 (PN3/SNS) in a rat model of visceral pain. J Neurosci 21:8690–8696.

Zhou XF, Zettler C, Rush RA (1994) An improved procedure for the immunohistochemical localization of nerve growth factor-like immunoreactivity. J Neurosci Methods 54:95–102.